

Nanoscale

Accepted Manuscript



This is an *Accepted Manuscript*, which has been through the Royal Society of Chemistry peer review process and has been accepted for publication.

Accepted Manuscripts are published online shortly after acceptance, before technical editing, formatting and proof reading. Using this free service, authors can make their results available to the community, in citable form, before we publish the edited article. We will replace this *Accepted Manuscript* with the edited and formatted *Advance Article* as soon as it is available.

You can find more information about *Accepted Manuscripts* in the [Information for Authors](#).

Please note that technical editing may introduce minor changes to the text and/or graphics, which may alter content. The journal's standard [Terms & Conditions](#) and the [Ethical guidelines](#) still apply. In no event shall the Royal Society of Chemistry be held responsible for any errors or omissions in this *Accepted Manuscript* or any consequences arising from the use of any information it contains.

1 **Simultaneous Direct Detection of Shiga-toxin Producing *Escherichia coli* (STEC) Strains**
2 **by Optical Biosensing with Oligonucleotide-functionalized Gold Nanoparticles**

3

4 Irwin A. Quintela¹, Benildo G. de los Reyes², Chih-Sheng Lin³, and Vivian C.H. Wu^{1*}

5

6 ¹ School of Food and Agriculture, The University of Maine, Orono, ME 04469-5735, USA,

7 ² School of Biology and Ecology, The University of Maine, Orono, ME, 04469-5735, USA,

8 ³ Department of Biological Science and Technology, National Chiao Tung University, Hsinchu
9 30005, Taiwan

10

11

12

13 * Corresponding author. Tel.: +1 207 581 3101; Fax: +1 207 581 1636

14 E-mail address: vivian.wu@umit.maine.edu

15

16 **Abstract**

17 A simultaneous direct detection of Shiga-toxin producing strains *E. coli* (STEC; “Big
18 Six” – O26, O45, O103, O111, O121, and O145) as well as O157 strains by optical biosensing
19 with oligonucleotide-functionalized gold nanoparticles (AuNPs) was developed.

20 Initially, conserved regions of *stx* genes were amplified by asymmetric polymerase chain
21 reaction (asPCR). Pairs of single stranded thiol-modified oligonucleotides (30-mer) were
22 immobilized onto AuNPs and used as probes to capture regions of *stx1* (119-bp) and/or *stx2*
23 (104-bp) genes from STEC strains. DNA samples from pure cultures and food samples were
24 sandwich hybridized with AuNP-oligo probes at optimal conditions (50°C, 30 min). A complex
25 was formed from the hybridization of AuNP-probes and target DNA fragment that retained
26 initial red color of the reaction solutions. For non-target DNA, a color change from red to
27 purplish-blue was observed following an increase in salt concentration, thus providing the basis
28 of simultaneous direct colorimetric detection of target DNA in the samples. Enrichment and
29 pooling systems were incorporated to efficiently process large number of food samples (ground
30 beef and blueberries) and detection of live targets.

31 The detection limit was < 1 log CFU/g, requiring less than 1 h to complete after DNA
32 sample preparation with 100% specificity. Gel electrophoresis verified AuNP-DNA
33 hybridization while spectrophotometric data and transmission electron microscope (TEM)
34 images supported color discrimination based on the occurrence of molecular aggregation. In
35 conclusion, the significant features of this approach took advantage of the unique colorimetric
36 properties of AuNPs as a low-cost and simple approach yet with high specificity for
37 simultaneous detection of STEC strains.

38 **Keywords:** gold nanoparticle; optical biosensing; STEC; Shiga-toxin

39 1. Introduction

40 The emergence of Shiga toxin-producing strains of *E. coli* (STEC) as a major foodborne
41 pathogen has posed serious public health concerns ¹. Epidemiological evidence shows that
42 specific STEC serotypes account for a large number of serious infections such as hemorrhagic
43 colitis and hemolytic-uremic syndrome ^{2,3}.

44 O-antigens on the surface of *E. coli* are significant virulence factors that are targets of
45 both innate and adaptive immune systems, playing a major role in pathogenicity. The antigenic
46 specificity of the strain is based on the O-antigens that determine the O-serogroups ⁴. The top six
47 O-groups (“Big Six” - O26, O45, O103, O111, O121, and O145) share common
48 epidemiological and virulence properties and have been determined by the Centers for Disease
49 Control and Prevention (CDC) to be the causative agents of 71% of non-O157 STEC diseases ³⁻⁶.
50 STEC strains release two putative potent cytotoxins called Shiga toxins (Stx1 and Stx2), encoded
51 by *stx1* and *stx2* genes, respectively ^{7,8}. There are more than 100 serotypes of STEC that carry
52 either or both *stx1* and *stx2* ⁹. With its low infectious dose, STEC strains can cause damages to
53 the intestinal linings, seizures, respiratory and kidney failures, and paralysis of susceptible
54 patients due to Shiga toxins ¹⁰. Recently, the top six serogroups have been declared by the U.S.
55 Department of Agriculture, Food Safety and Inspection Service (USDA FSIS) to be adulterants
56 in raw beef ¹¹. Aside from beef, STEC are also transmitted through a wide array of foods
57 including dairy products and fresh produce such as lettuce and spinach ^{12,13}. One of the most
58 extensive STEC outbreaks occurred in Germany on May 2011 with 3,816 cases, 845 of which
59 had HUS and 54 deaths were recorded ¹⁴.

60 To efficiently detect STEC contamination in food and environmental samples, the assay
61 should be easy, quick and accurate. The traditional culture method using Sorbitol MacConkey

62 agar is relatively inexpensive, effective, and widely used based on the absence of sorbitol
63 fermentation. However, the long turnaround time and non-specificity due to the emerging non-
64 O157 STEC strains that ferment sorbitol limit its use⁹. Conventional PCR assays are flexible in
65 terms of detection and identification of multiple target genes in one reaction. However, most
66 first-generation PCR assays have cumbersome protocols for detecting the amplified products and
67 numerous PCR assays lack sequence specific identification of the amplified genes¹⁵. None-
68 portable PCR systems make the application difficult in the on-site testing. Discriminating viable
69 from non-viable cells after PCR is another challenge because DNA is always present whether the
70 cell is dead or alive¹⁶.

71 Optical biosensors have received substantial interest for bacterial pathogen detection due
72 to its simplicity, sensitivity, and selectivity. Target recognition usually generates electrical or
73 optical signals, which can ultimately report the presence of the target materials¹⁷. Gold
74 nanoparticles (AuNPs) are emerging novel colorimetric reporters for the detection of various
75 substances such as nucleic acids, proteins, and antibodies due to its excellent optical, physical
76 and chemical properties such as high dispersity in solution, ease of synthesis, low cost, and
77 extremely high extinction coefficients (hundreds to thousand larger than those of organic dyes)¹⁸.
78 AuNPs are spherical particles with a typical diameter of 2 – 50 nm that exhibit distinctive
79 properties known as Surface Plasmon Resonance (SPR) or the collective electron oscillations
80 which give intense red color and allows shifting to blue color upon aggregation of AuNPs^{19,20}.
81 This color change offers a suitable platform for colorimetric sensing of any specific analyte of
82 interest²¹. The sensitivity and selectivity of AuNPs based colorimetric detection are comparable
83 to fluorescent detection methods²². Though immunoassays and other molecular based biosensing
84 methods have been widely studied to rapidly detect and identify foodborne bacterial pathogens,

85 many of these methods are designed for detection of a single species of pathogens in one assay
86 ²³. Therefore, a simultaneous method that will detect and identify STEC strains from food and
87 environmental samples is highly desirable.

88 Our aim was to develop a method for simultaneous direct detection of STEC strains by an
89 optical biosensing method with oligonucleotide-functionalized AuNPs and DNA sandwich
90 hybridization. To our knowledge, this is the first report of a simultaneous and highly sensitive
91 optical biosensing detection method for the STEC strains that express and produce either *stx1* or
92 *stx2* or both.

93

94 **2. Experimental methods**

95 **2.1. Bacterial cultures preparation**

96 Twenty STEC strains representing seven serogroups, O26:H11 HH8, O26:H11 SJ1,
97 O26:H11 SJ2, O26:H2 TB285, O45:H2 SJ7, O45:H2 05-6545, O45:H2 96-3285, O103:H2 GG7,
98 O103:H25 SJ11, O103:H11 SJ12, O111:H8 EE5, O111:NM SJ13, O111:H- 94-0961, O121:H19
99 SJ18, O121:H19 96-1585, O145:NM SJ23, O145:H28 07865, O145:H- 94-0491, O157:H7
100 (ATCC 35150), O157:H7 (ATCC 49835) and *S. Typhimurium* H3379, were obtained from the
101 U.S. Department of Agriculture – Agricultural Research Service, Eastern Regional Research
102 Center (Wyndmoor, PA, USA) and from the Pathogenic Microbiology Laboratory at the
103 University of Maine . Bacterial cells were stored in cryogenic beads with Brucella broth and
104 glycerol (CryoSavers; Hardy Diagnostics, Santa Maria, CA, USA) at -80°C . Frozen culture
105 beads were activated by incubating overnight at 37°C in Brain Heart Infusion (BHI) broth
106 (Neogen, Lansing, MI, USA). Revived cells were re-inoculated to new BHI broth under the same

107 conditions to prepare the working cultures. Viable cell counts during the experiments were
108 obtained by plating on MacConkey Agar with Sorbitol (Neogen).

109 **2.2. Primers and probes designs**

110 Two pairs of *stx* specific primers [For(*stx1-1-F*)- (5'-CATCGCGAGTTGCCAGAATG-
111 3') and Rev(*stx1-1-R*)- (5'-AATTGCCCCCAGAGTGGATG- 3'); For(*stx2-5-F*)- (5'-GTATAC
112 GATGACGCCGGGAG- 3') and Rev(*stx2-5-F*)- (5' -TTCTCCCCACTCTGACACCA- 3')
113 were designed using NCBI Primer Blast to amplify the conserved regions of *stx1* (119-bp) and
114 *stx2* (104-bp) genes. Primer sequences were synthesized by Integrated DNA Technologies
115 (Coralville, IA, USA).

116 Oligonucleotide probes were manually designed based on sequence complementarity
117 with the target regions. Hybridization conditions for each probe with target *stx* region were
118 initially optimized and confirmed by digesting the hybridization products with S1 Nuclease
119 (Promega, Madison, WI, USA). Probes were modified with thiol-linked tags [HS-(CH₂)₆] at the
120 5' or 3' terminus, [P1-30-119AS-SH - (5'- CCGGACACA TAGAAGGAAACTCATCAGATG
121 - 3'-(CH₂)₆-HS) and P2-30-119AS-SH - (HS-(CH₂)₆ - 5'-TTTATTGTGCGTAATCCCACGG
122 ACTCTTCC - 3'); P1-30-104AS-SH - (5'-ATTCGCCCC CAGTTCAGAGTGAGGTCCACA -
123 3'-(CH₂)₆-HS) and P2-30-104AS-SH - (HS-(CH₂)₆ - 5'-CCTCTCCCCGATACTC
124 CGGAAGCACATTGC - 3') (Eurogentec, San Diego, CA, USA).

125 **2.3. DNA extraction and asymmetric PCR**

126 Genomic DNA from pure bacterial cultures (concentration levels at 1 – 3 CFU/ml) was
127 harvested using DNeasy Blood & Tissue Kit according to manufacturer's protocol (Qiagen
128 GmbH, Hilden, Germany); 2 µl of DNA samples from the final elution step were used as
129 templates for asymmetric PCR (asPCR). All DNA samples were stored at -20°C until use.

130 The optimized asPCR conditions that amplified the 119-bp target region of *stx1* and 104-
131 bp region of *stx2* had an initial denaturation at 95°C for 2 min; 35 cycles of 30 sec denaturation
132 at 95°C, annealing at 56°C for 30 sec, elongation at 72°C for 30 sec and final extension at 72°C
133 for 5 min. The same protocol was used for genomic DNA extraction and amplification of target
134 regions from different food enrichments.

135 **2.4. Synthesis of AuNPs**

136 An average of 13 nm diameter of AuNPs was synthesized using citrate reduction method
137 with slight modifications as previously described²⁴. Briefly, 25 ml of 2.5 mM of chloroauric acid
138 solution was brought to 130°C with constant stirring. Sodium citrate (3 ml of 38.3 mM) was
139 rapidly injected to the boiled chloroauric acid. The solution was moderately stirred for another
140 10 min at room temperature. Then, the freshly prepared AuNPs was characterized by measuring
141 its absorption spectra (400 – 700 nm wavelength) using a microplate reader spectrophotometer
142 (BioTek Power Wave XS, Winoskii, VT, USA).

143 **2.5. Functionalization of AuNPs with thiol-modified oligonucleotide probes**

144 AuNPs solution was transferred to centrifuge tubes wrapped with aluminum foil. Each
145 thiol-modified oligonucleotide probe (20 μM, 20 μl) was added to the AuNPs solution (20 μM,
146 980 μl) and kept in water bath at 37°C for 24 h²⁴. Increasing amount of salt buffer solution (0.05
147 – 1.0 M NaCl in 10 mM Na₂HPO₄, pH 7.4) was added at six different time points for the next 48
148 h to steadily immobilize the probes onto the surface of AuNPs. The excess unbound probes were
149 washed from the functionalized AuNP solution by centrifugation at 19,530 × g for 30 min. The
150 resulting clear supernatant was carefully removed while the remaining dark red oily residue was
151 dispersed in 0.05 M NaCl in 10 mM Na₂HPO₄, pH 7.4. Final absorption spectra was measured

152 (400 – 700 nm wavelength) using a microplate reader spectrophotometer (BioTek Power Wave
153 XS, Winoskii, VT, USA). Functionalized AuNP solution was stored at 4°C until further use.

154 **2.6. AuNP optical biosensing for STEC strains**

155 Figure 1 presents the principles of the AuNPs optical biosensing based on DNA sandwich
156 hybridization using functionalized AuNPs. AuNP-probes (50 µl each) and its corresponding
157 target and non-target asymmetric PCR products were denatured separately and iced for 5 min.
158 Denatured probes and PCR products were mixed together and incubated at 50°C for 30 min to
159 complete the hybridization process. The reaction solutions were kept at room temperature for 5
160 min before the color challenge test.

161 Salt solution (1 M NaCl in 10 mM Na₂HPO₄, pH 7.4, in the final reaction) was added to
162 each reaction solution for examination of color reaction. For quantitative analysis, absorption
163 spectra was measured (400 – 700 nm wavelength) before and after adding salt solution using a
164 microplate reader spectrophotometer (BioTek Power Wave XS, Winoskii, VT, USA). For
165 verification of successful DNA and AuNP-probes hybridization, reaction solutions (20 µl each)
166 were run in gel electrophoresis (3% agarose gel and ethidium bromide) prior to adding salt
167 solution.

168 **2.7. Transmission electron microscopy (TEM)**

169 Philips CM10 TEM (Philips, Eindhoven, Netherlands) operating at 80kV was used to
170 characterize AuNPs. Briefly, 2 µl of each thiol-modified AuNPs samples (with or without
171 bacterial sample) was deposited onto a carbon-coated grid (200 mesh). The grids were then
172 allowed to air dry at room temperature for 30 – 45 min before viewing under TEM for analysis.

173 **2.8. Detection of STEC from food samples**

174 **2.8.1. Pooling enrichment**

175 Ground beef and blueberries were used to assess the application of the developed AuNP
176 optical biosensing in STEC contaminated food matrices. Pooling and enrichment systems (Figure
177 2) were incorporated to efficiently process a large number of food samples (50 samples) at the
178 shortest possible time and ensure detection of viable STEC cells. The initial microbial
179 contamination level in food samples before enrichment was $< 1 \log \text{CFU/g}$, which was achieved
180 by 10-fold serial dilution and confirmed by the plate count method with MacConkey Agar with
181 Sorbitol (Neogen).

182 **2.8.2. Ground beef**

183 Ground beef was purchased from a local retail store and used to prepare inoculated
184 samples. The procedures for identifying STEC in the USDA/Food Safety and Inspection Service
185 (FSIS) Microbiology Laboratory Guidebook (MLG) 5.05 were adapted with slight modification.
186 Briefly, 50 samples (25 g each) were collected and grouped into five; each group had 10
187 samples. Freshly grown cells of STEC strains - O26:H11 HH8, O26:H11 SJ1, O26:H11 SJ2,
188 O26:H2 TB285, O45:H2 SJ7, O45:H2 05-6545, O45:H2 96-3285, O45:H2 SJ7, O45:H2 05-
189 6545, O45:H2 96-3285, O103:H2 GG7, O103:H25 SJ11, O103:H11 SJ12, O111:H8 EE5,
190 O111:NM SJ13, O111:H- 94-0961, O121:H19 SJ18, O121:H19 96-1585, O145:NM SJ23,
191 O145:H28 07865, O145:H- 94-0491, O157:H7 (ATCC 35150) and O157:H7 (ATCC 49835)
192 were spiked randomly at $0 - 9 \text{CFU/g}$ ($< 1 \log \text{CFU/g}$) contamination levels. Each sample was
193 transferred into individual stomacher bag (Blender Bag, Fisher Scientific, Wilmington, DE,
194 USA). A volume of 225 ml of modified Tryptic Soy Broth (mTSB) with 8 mg/l novobiocin and
195 casamino acids (Neogen) was added and then homogenized using a stomacher for 2 min. All pre-
196 enriched samples were incubated at $42 \pm 1^\circ\text{C}$ for 6 h.

197 Fifty ml aliquot was collected from each post-enriched sample and pooled together as
198 shown in Figure 2. To remove solidified fats and debris, 1 ml aliquots from each of the five
199 pooled samples were centrifuged at low speed ($125 \times g$) for 10 min. Supernatant was then
200 filtered through 5 μm pore size membrane (Acrodisc, Pall Corporation, Cornwall, UK). Genomic
201 DNA was extracted with the DNeasy Blood & Tissue Kit (Qiagen) according to manufacturer's
202 protocol.

203 **2.8.3. Blueberries**

204 Blueberries were supplied by a local farmer in Maine. Briefly, 50 samples (25 g each)
205 were collected and grouped into five; each group had 10 samples. Freshly grown cells of same
206 STEC strains as used in the ground beef inoculation were spiked individually to 2 groups at 0 – 9
207 CFU/g ($< 1 \log \text{CFU/g}$) contamination levels. Briefly, 50 samples (25 g each) of blueberries
208 were prepared in stomacher bag (Blender Bag, Fisher Scientific, Wilmington, DE, USA). Then,
209 225 ml of mTSB with 8 mg/l novobiocin and casamino acids (Neogen) was added and mixed
210 (Rotomix Orbital Shaker, Dubuque, IA, USA) at $2 \times g$ for 2 min. Similar to ground beef, all pre-
211 enriched samples were incubated at $42 \pm 1^\circ\text{C}$ for 6 h.

212 From each post-enriched sample, 50 ml was collected and pooled together as shown in
213 Figure 2. Genomic DNA was extracted from each these five blueberry pooled samples using
214 DNeasy Blood & Tissue Kit (Qiagen) as described by the supplier.

215 **2.9. AuNP optical biosensing on food samples**

216 After genomic DNA extraction and target amplification, procedures for AuNP optical
217 biosensing of various STEC pure culture strains (described in Section 2.6) were applied to food
218 samples in duplicates using 96-well microplate. In addition, 1 log CFU/ml contamination level
219 for both positive (STEC O145:NM) and negative (*S. Typhimurium* H3379) controls and blank

220 (nuclease-free water) were included. AuNP optical biosensing was conducted in parallel with
221 conventional PCR and gel electrophoresis for direct comparison.

222 **2.10. Statistical analysis**

223 The experimental data were analyzed using JMP software. Each experiment was repeated
224 three times to test the reproducibility and stability of the AuNP optical biosensors. Mean \pm
225 standard deviation (S.D.) absorbance reading of reaction mixtures after adding salt-buffer
226 solution in experiments were compared by a two-tailed Student's *t*-test. *P*-values less than 0.05
227 were considered to be statistically significantly different.

228

229 **3. Results and Discussion**

230 **3.1. Functionalization of AuNPs with thiol-modified oligonucleotide probes**

231 AuNPs are unique kinds of hybrid materials due to their characteristic optical properties
232 that allow convenient signal transduction for biosensor applications facilitated by the
233 colorimetric changes of dispersed and aggregated particles. AuNPs obtained by the citrate
234 reduction method appear as monodispersed globular structures with a diameter of about 10 – 15
235 nm, stabilized by weakly bound citrate anions^{20,25}. AuNPs with approximately 13 nm diameter
236 absorb green light, which corresponds to a strong absorption band (surface plasmon band) at
237 ~520 nm in the visible light spectrum; therefore solutions of AuNPs appear red in color²⁶. The
238 surface of AuNPs can be tailored by the functionalization of ligands (oligonucleotides and
239 proteins) to specifically bind with its target. The freshly synthesized AuNPs synthesized in the
240 present study were functionalized with thiol-modified oligonucleotides.

241 Increased salt-buffer concentration during the immobilization of thiol-modified
242 oligonucleotide on the surface of AuNPs reduces electrostatic repulsion between negatively-

243 charged strands due to a screening effect permitting more oligonucleotides to approach the
244 particle surface²⁷. Thiol modification on the 5' end of one probe and 3' end of the other probe
245 provides stable chemical bonds between the thiol group and gold atoms efficiently replacing
246 citrate ions on the surface of AuNPs and enhancing immobilization^{10, 25}.

247 Successful immobilization of thiol-modified oligonucleotide probes caused shift of 3 – 5
248 nm on its absorbance peak of AuNP solution without noticeable change in color. Optimization
249 steps in the experiment were performed by adjusting the amount and volume ratio of thiol-
250 modified oligonucleotide and AuNPs during the immobilization process. Washing of
251 functionalized AuNPs after immobilization step was also incorporated in the protocol to ensure
252 that unbound thiol-probes were eliminated in the final AuNP-probe solution prior to DNA
253 sandwich hybridization. These steps have significantly reduced the background noise and greatly
254 enhanced the color reactions of samples after subjecting to an increased salt concentration. The
255 optimized final concentration of functionalized AuNPs was 20 nM (Supplementary information).

256 **3.2. AuNPs optical biosensing for STEC strains in pure cultures**

257 DNA samples from different log concentrations of cells (1 – 3 log CFU/ml) were used for
258 asPCR. The specificity of the assay was demonstrated by precise amplification of *stx* genes from
259 STEC strains of different serogroups. By using asPCR, single stranded amplicons were generated
260 corresponding to the highly-conserved *stx* target regions (119-bp/*stx1* and 104-bp/*stx2*).

261 The AuNP optical biosensing was developed and applied to the amplified regions of
262 *stx1/stx2* genes from various STEC strains. Twenty STEC strains representing the “Big Six” and
263 O157 serogroups were tested with the negative control (non-target, *S. Typhimurium* H3379) and
264 blank (nuclease-free water instead of DNA). In a 96-well microplate, it was observed that the
265 DNA sample reactions from various STEC strains remained were red in color whereas those

266 containing *S. Typhimurium* H3379 and blank solutions developed a purplish-blue color after the
267 addition of salt (1 M, final reaction concentration). This approach allowed simultaneous visual
268 comparison of solutions before and after the salt induced AuNP-probes aggregation. Purification
269 steps of amplified products were found not to be necessary since 35 cycles of asPCR provided an
270 adequate amount of detectable single-stranded DNA.

271 As shown in Figure 3A, AuNP optical biosensing targeting *stx1* gene of STEC O26: H11
272 and *stx2* gene of STEC O111:H19 strains, hybridization of AuNP-probes with both target regions
273 retained its initial red color. This was due to the formation of AuNP-probes network complexes
274 that stabilized AuNPs even in an increased salt concentration. The negatively-charged phosphate
275 groups of DNA backbone of the newly formed AuNP-probes complexes enhanced interparticle
276 electrostatic repulsion force. This repulsion force effectively counteracted both van der Waals
277 attraction force of AuNPs and high ionic strength of salt solution²⁸. Moreover, the formation of
278 DNA duplex from DNA sandwich hybridization may have provided a buffering effect to the
279 reaction solution, thereby stabilizing AuNPs and prevented it from aggregating in an increased
280 salt environment²⁴. For the negative control reaction solution containing AuNP-probes and non-
281 complementary sequences, a changed from red to purplish-blue color was observed. DNA
282 sandwich hybridization did not occur in the negative control, thus, only a weak repulsion force
283 between AuNPs was present which made it prone to destabilization. As salt solution was added,
284 the net ionic strength of the negative reaction solution increased that reduced and neutralized the
285 existing weak interparticle repulsion charge of AuNPs. The increased in salt concentration
286 ultimately resulted to the aggregation of AuNPs and change in color of the negative control
287 samples.

288 Spectrophotometric data curve presented in Figure 3B illustrates the broadening of peaks
289 towards longer wavelength for the non-target and blank reaction solutions due to particles
290 aggregation after adding salt solution. For target samples, the absorbance curves after adding salt
291 (1 M in final reaction) peaked at a lower absorbance compared to its initial absorbance due to the
292 additional volume of salt solution which diluted the reaction solutions. However, it did not alter
293 the trend of color reactions between target and non-target samples. The extent of this shift
294 depends mainly on particle and aggregate sizes, density, fractal dimensions, whereas the rate of
295 change of the spectral shift depends on aggregate size and growth rate²⁰. Figure 3D shows the
296 successful DNA sandwich hybridization between AuNP-probes and target DNA on gel
297 electrophoresis, while the negative control and blank reaction did not show any band. This figure
298 presents results that perfectly correlate with the results of AuNP optical biosensing assay
299 reactions as described. In this study, an aggregation parameter was derived to quantify the
300 variation of integrated absorbance of samples after adding salt solution. The absorbance ratio
301 (625 nm/525 nm) of the non-target samples and blank from two longer wavelengths, as presented
302 in Figures 3C, 4C, 4D and 5B clearly shows significant difference at $P < 0.05$ as compared to the
303 target samples. These results confirmed the occurrence of salt induced AuNP-probes aggregation
304 that allowed discrimination between STEC and non-STEAC strains.

305 Figures 3E, 3F and 3G show TEM images of AuNP-probes in various reaction solutions
306 after an increased salt concentration (1M in final reaction). Figure 3E is an image of AuNP-
307 probes and non-target DNA from *S. Typhimurium* H3379 (1 log CFU/ml) showing the
308 aggregation of AuNPs as interparticle electrostatic repulsion is relieved by increasing salt
309 concentration. Both Figure 3F (STEC O26 – *stx1* assay) and Figure 3G (STEC O111 – *stx2*
310 assay) present successfully hybridized AuNPs-probes with complementary target sequences in an

311 increased salt concentration reaction solution. The images show well dispersed and highly
312 stabilized AuNPs.

313 To further demonstrate the reproducibility and stability of the assay, the STEC strains
314 carrying both *stx* genes can be tested. Figure 4 presents a successful detection of both *stx1* and
315 *stx2* genes from STEC O145:NM targeting in a range of 1 – 3 logs CFU/ml bacterial source.
316 Figure 5 shows simultaneous detection of *stx1* and *stx2* genes from STEC O45:H2, STEC
317 O103:H11, STEC O121:H19 and STEC O157:H7 at 1 log CFU/ml pure culture set-up.

318 Earlier results (data not shown) demonstrated 100% specificity of the assay in
319 simultaneous and direct detection of asPCR products from 9 log CFU/ml STEC cell
320 concentration while employing *S. Typhimurium* and nuclease-free water as the negative control
321 and blank, respectively. These results provided the basis to challenge the sensitivity of the assay
322 by using lower cell concentrations (1 – 3 logs CFU/ml) for DNA preparation. Based on the
323 results shown in Figures 3 – 5, the limit of detection (LOD) of the assay is 1 log CFU/ml.

324

325 **3.3. AuNP optical biosensing on food samples**

326 STEC is a rapidly emerging threat as a stubborn foodborne pathogen and together with *E.*
327 *coli* O157:H7, it has been implicated with hemorrhagic colitis and potentially deadly systemic
328 sequelae in humans²⁹. However, STEC detection in most end-product testing is primarily
329 focused on STEC O157:H7, and screening of other serogroups or strains is often neglected³⁰.
330 The applicability of the simultaneous detection of STEC strains with the developed AuNP
331 optical biosensing method was evaluated in ground beef and blueberries. Prevalence of STEC
332 contamination in these food samples was also assessed.

333 Combined with a robust sampling plan and shortened enrichment procedures, the new
334 AuNP optical biosensing method was effective in detecting contaminants in ground beef and
335 blueberries that were experimentally inoculated with various concentrations of STEC cells with
336 < 9 CFU/g. Enrichment and pooling systems were incorporated to efficiently process large
337 number of food samples at the shortest possible time and ensure detection of viable STEC cells.
338 In the present study, 6 h enrichment was determined by plate count method (data not shown) to
339 be the shortest period that would ensure growth of STEC strains to > 1 log CFU/g. Modified
340 TSB with 8 mg/l novobiocin and casamino acids (Neogen) was used to enrich food samples with
341 low levels of STEC and to increase the probability of harvesting and extracting genomic DNA
342 for asPCR.

343 Two out of five post-enriched pooled samples (data not shown), either ground beef or
344 blueberries, tested positive for the presence of STEC strains by the AuNP optical biosensing in a
345 96-well microplate. A total of forty individual post-enriched samples which were components of
346 positive pools were then tested simultaneously. Duplicate reaction samples in a 96-well
347 microplate after adding salt are shown in Figure 6. Individual STEC strain may carry one or both
348 types of *stx* genes commonly contaminating ground beef and other food items including leafy
349 greens, thus duplicate samples ensure greater detection coverage⁹. In total, 33 samples were
350 positive for *stx1* and 25 samples for *stx2* from both ground beef and blueberries samples. Thirty-
351 seven samples were positive for both *stx* genes while 22 samples showed negative detection.

352 With the blank and negative control (*S. Typhimurium*) turned purplish-blue after adding
353 salt solution, all positive individual samples along with the positive control (STEC O145:NM)
354 were differentiated with ease. Color change for blank and non-target samples was observed
355 within 1 – 2 min after adding salt solution. Without the aid of any complicated instrument,

356 conducting visual examination to simultaneously discriminate negative and positive reactions
357 from the samples offers flexibility and rapid detection³¹. AuNP optical biosensing was compared
358 with conventional PCR and gel electrophoresis showing similar results. Reference to the
359 concentration of STEC strains inocula, the data presented confirmed $< 1 \log$ CFU/g detection
360 limit for the AuNP optical biosensor in food samples. This detection limit is very significant
361 based on the previous study that the infectious dose of STEC strains such as STEC O157:H7 is $<$
362 10 cells¹⁰. The actual DNA sandwich hybridization steps and color challenge test require less
363 than 1 h to complete. Shorter turnaround detection period while accommodating multiple
364 samples translates convenience and automation³². This feature makes this newly developed
365 optical biosensing advantageous over the other common approaches especially for screening
366 STEC in food samples when rapid testing with immediate results is highly sought. In the present
367 study, the detection subjects come from the amplified DNA (*stx* genes) of pre-enriched STEC
368 cells in pure culture or inoculated samples. It was not intended to provide a precise correlation
369 between the value 625 nm/525 nm ratio and the original concentration of STEC (Supplementary
370 information).

371 Currently, numerous methods utilizing AuNPs for detection are available as discussed
372 and reviewed by several researchers. AuNP-based optical biosensing detection method still
373 continues to be a promising tool for rapid and specific foodborne pathogen detection. It has been
374 presented in this study the unique and stable properties of AuNPs that can be exploited for
375 simultaneous pathogen detection while considering the ease of its synthesis and as an
376 inexpensive material. The advantageous features of this approach successfully challenged a
377 superior detection limit in pure culture and actual food samples. More importantly, this study has
378 incorporated simplified sampling approach and enrichment method that made the entire protocol

379 turnaround time to be less than a day and ensured the viable cell detection. All steps established
380 in this study require simple equipment and do not need highly skilled staff.

381

382 **4. Conclusions**

383 In this study, a direct and simultaneous detection of STEC strains by an optical
384 biosensing method using oligonucleotide-functionalized AuNPs was developed. This approach
385 allowed a simultaneous visual discrimination and identification of STEC DNA samples
386 following DNA sandwich hybridization with highly specific thiol-modified probes immobilized
387 on the surface of AuNPs and optimum salt concentration (1 M in final reaction). To demonstrate
388 the stability and reproducibility of this optical biosensing, the method was applied to artificially
389 inoculate pooled and individual ground beef and blueberries samples. The results showed that the
390 new biosensing assay is highly sensitive and stable for simultaneous and rapid detection of the
391 STEC strains carrying *stx* gene(s). The detection limit was superior ($< 1 \log \text{CFU/g}$) requiring
392 less than 1 h to complete after DNA sample preparation and 100% specificity. Gel
393 electrophoresis confirmed AuNP-DNA hybridization while spectrophotometric data and
394 transmission electron microscope (TEM) images supported the color discrimination based on the
395 occurrence of molecular aggregation. . The significant features of this approach took advantage
396 of the unique colorimetric properties of AuNPs as a low-cost, specific, and simple approach for
397 simultaneous detection of STEC strains, elevating the potential of nanobiosensing for rapid
398 detection of multiple foodborne pathogens to a different stage.

399

400

401

402 Acknowledgements

403 This research was supported by USDA NIFA-AFRI Competitive Grant (Award # 2011-
404 68003-30420) and the Maine Agricultural and Forest Experiment Station at the University of
405 Maine with external publication number 3680. This work is based upon research supported in
406 part by Hatch Grant number ME08562-10 from the USDA National Institute of Food and
407 Agriculture. The authors would like to thank Dr. Pina Fratamico, ERCC, ARS-USDA for
408 providing the STEC strains, Ms. Ai Kitazumi for her assistance during the initial part of the
409 experiment and Ms. Fang-Yuan Yeh (Cammy) for her input on the final layout of the figures.
410

411 **Figure Legends**

412 **Figure 1.** A schematic diagram of simultaneous direct detection of various STEC strains using
413 AuNP optical biosensing assay targeting *stx1* and *stx2* genes at optimized conditions (37°C for
414 30 min). **(A)** For target DNA set-up, a successful DNA sandwich hybridization between AuNP-
415 probes (Probe 1 and Probe 2) and target DNA occurs due to its high complementarity. Following
416 an increased salt concentration, AuNP-probes and target DNA complexes remain stable and
417 retain its original red color. **(B)** For non-target DNA (including blank) set-up, successful
418 hybridization does not occur but instead, salt-induced AuNP aggregation followed after
419 increasing its salt concentration. The color of reaction solutions with salt-induced aggregated
420 AuNPs shifts from the original red to purplish-blue. Color differentiation facilitates direct
421 detection of positive and negative samples. **(C)** For simultaneous direct detection of various
422 STEC strains using a 96-well microplate, each sample was prepared in duplicates for both *stx1*
423 and *stx2* assays. **(D)** A TEM image of oligonucleotide-modified AuNPs, 275,000 X
424 magnification.

425

426 **Figure 2.** The principles of rapid enrichment of STEC cells in food samples after artificial
427 inoculation, pooling and AuNP optical biosensing assay. **(A)** Simultaneous direct detection of
428 various STEC strains from ground beef (25 g) and blueberries (25 g) starts from the shortened
429 pre-enrichment using 225 ml modified Tryptic Soy Broth (mTSB) with 8 mg/l novobiocin and
430 casamino acids at $42 \pm 1^\circ\text{C}$ for 6 h to ensure detection of viable STEC cells. **(B)** Pooling of post-
431 enriched samples is performed to accommodate large number of food samples. **(C)** Amplified
432 samples generated by asymmetric PCR are simultaneously tested using AuNP optical biosensing
433 assay. **(D)** If pooled sample is tested negative, then all of its individual samples are declared

434 negative. (E) However, positive pooled sample requires testing of all its individual post-enriched
435 samples. Simultaneous AuNP optical biosensing assay is conducted in a 96-well microplate; gel
436 electrophoresis and spectrophotometric data confirm successful DNA sandwich hybridization.

437

438 **Figure 3.** Simultaneous direct detection of *stx1* gene from STEC O26:H11 strain and *stx2* gene
439 from STEC O111:H19 strain. In this pure culture set-up, each strain carries only one type of *stx*
440 gene. (A) AuNP optical biosensing assay before and after adding salt solution (50 μ l, 1 M NaCl-
441 Na₂HPO₄ final reaction). (B) Absorbance curve of representative samples before and after adding
442 salt (1 M NaCl-Na₂HPO₄ in final reaction) was generated showing the formation of new
443 absorbance peaks at longer wavelengths of non-target and blank samples. (C) Absorbance ratio
444 of samples at wavelengths 625 nm and 525 nm after adding salt (1 M NaCl-Na₂HPO₄ in final
445 reaction) shows significance difference at $P < 0.05$ between STEC strains, non-target and blank
446 samples which validated 1 log CFU/ml as the limit of detection (LOD). B = blank; NT = non-
447 target *S. Typhimurium* H3379 (1 log). (D) Gel electrophoresis was conducted to verify the
448 occurrence of a successful DNA sandwich hybridization between AuNP-probes and the target
449 gene. Gel bands are shown at the expected 119-bp (*stx1*) and 104-bp (*stx2*) regions, respectively.
450 All samples were in log CFU/ml concentration. (E) A TEM image of AuNP-probes and non-
451 target DNA from *S. Typhimurium* H3379 (1 log CFU/ml) clearly shows aggregation of AuNPs
452 as interparticle electrostatic repulsion force is relieved by increasing salt concentration. (F)
453 STEC O26 1log CFU/ml – *stx1* assay and (G) STEC O111 1log CFU/ml – *stx2* assay present
454 successfully hybridized AuNPs-probes with complementary target sequences in an increased salt
455 concentration reaction solutions. AuNP-probes are obviously linked with each other but not

456 tightly bound. The last two images both show well dispersed and highly stabilized AuNPs.

457 Inserts on the upper right corner of each image are the actual AuNPs reaction solutions.

458

459 **Figure 4.** Simultaneous and direct detection of *stx1* and *stx2* genes from STEC O145:NM at 1

460 log CFU/ml, 2 log CFU/ml and 3 log CFU/ml pure culture set-up. STEC O145:NM carries both

461 *stx1* and *stx2* genes. (A) AuNP optical biosensing assay for *stx1* gene. (B) AuNP optical

462 biosensing assay for *stx2* gene. Absorbance ratio of samples at wavelengths 625 nm and 525 nm

463 after adding salt (1 M NaCl-Na₂HPO₄ in final reaction) is presented in for *stx1* assay (C) and for

464 *stx2* assay (D), indicating significance difference at $P < 0.05$ between STEC strain, non-target

465 and blank samples. B = blank; NT = non-target *S. Typhimurium* H3379. All samples were in log

466 CFU/ml concentration.

467

468 **Figure 5.** Simultaneous direct detection of both *stx1* and *stx2* genes from STEC O45:H2, STEC

469 O103:H11, STEC O121:H19 and STEC O157:H7 at 1 log CFU/ml pure culture set-up. Each

470 strain is carrying both genes. (A) AuNP optical biosensing assay before and after adding salt

471 solution (50 μ l, 1 M NaCl-Na₂HPO₄ final reaction). (B) Absorbance ratio of samples at

472 wavelengths 625 nm and 525 nm after adding salt (1 M NaCl-Na₂HPO₄ in final reaction)

473 indicating significance difference at $P < 0.05$ between STEC strains, non-target and blank

474 samples. B = blank; NT = non-target *S. Typhimurium* H3379. All samples were in 1 log CFU/ml

475 concentration.

476

477 **Figure 6.** Application of the newly-developed AuNP optical biosensing assay on artificially

478 inoculated food samples. Individual ground beef (20 samples) and blueberries (20 samples) from

479 positive post-enriched pooled samples, in duplicates, were simultaneously tested for STEC
480 strains in a 96-well microplate. The figure shows the reaction solutions following an increased in
481 salt concentration (1 M NaCl-Na₂HPO₄ in final reaction). Wells A1-A3 and E1-E3 contain blank,
482 negative (*S. Typhimurium* H3379) and positive controls (STEC O145:NM), respectively. In
483 total, 33 samples showed positive detection for *stx1*, 25 samples for *stx2* and 37 samples for both
484 *stx1* and *stx2*. Twenty-two samples showed negative detection for *stx1* and *stx2*.

485

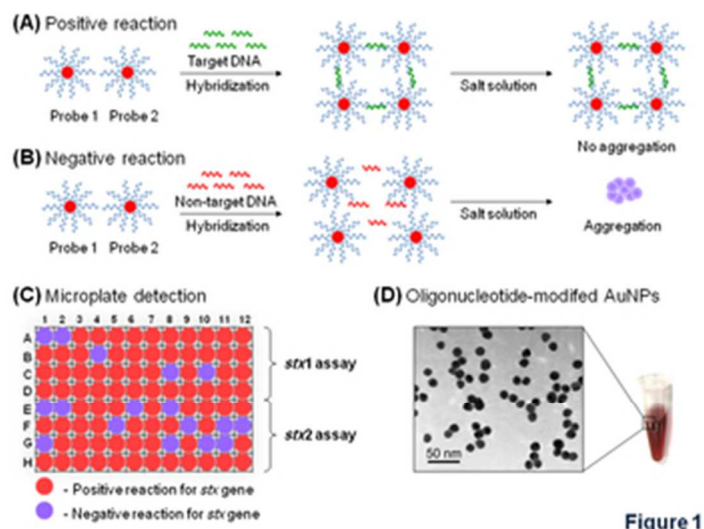
486

487

References

- 488
489
490 1. D. G. Newell, M. Koopmans, L. Verhoef, E. Duizer, A. Aidara-Kane, H. Sprong, M.
491 Opsteegh, M. Langelaar, J. Threfall, F. Scheutz, J. v. der Giessen and H. Kruse, *Int. J. Food*
492 *Microbiol.*, 2010, 139, Supplement, S3-S15.
- 493 2. A. W. Paton and J. C. Paton, *J. Clin. Microbiol.*, 2002, 40, 271-274.
- 494 3. F. Wang, L. Jiang, Q. Yang, W. Prinyawiwatkul and B. Ge, *Appl. Environ. Microbiol.*, 2012,
495 78, 2727-2736.
- 496 4. C. DebRoy, E. Roberts, A. M. Valadez, E. G. Dudley and C. N. Cutter, *Foodborne Pathog.*
497 *Dis*, 2011, 8, 651-652.
- 498 5. J. T. Brooks, E. G. Sowers, J. G. Wells, K. D. Greene, P. M. Griffin, R. M. Hoekstra and N.
499 A. Strockbine, *J. Infect. Dis.*, 2005, 192, 1422-1429.
- 500 6. N. Kalchayanand, T. M. Arthur, J. M. Bosilevac, J. W. Schmidt, R. Wang, S. D. Shackelford
501 and T. L. Wheeler, *J. Food Prot.*, 2012, 75, 1207-1212.
- 502 7. J. E. Blanco, M. Blanco, M. P. Alonso, A. Mora, G. Dahbi, M. A. Coira and J. Blanco, *J.*
503 *Clin. Microbiol.*, 2004, 42, 311-319.
- 504 8. W. M. Fedio, K. C. Jinneman, K. J. Yoshitomi, R. Zapata, C. N. Wendakoon, P. Browning
505 and S. D. Weagant, *Int. J. Food Microbiol.*, 2011, 148, 87-92.
- 506 9. T. E. Gryns, L. M. Sloan, J. E. Rosenblatt and R. Patel, *J. Clin. Microbiol.*, 2009, 47, 2008-
507 2012.
- 508 10. V. C. Wu, S.-H. Chen and C.-S. Lin, *Biosensors Bioelectron.*, 2007, 22, 2967-2975.
- 509 11. G. E. Tillman, J. L. Wasilenko, M. Simmons, T. A. Lauze, J. Minicozzi, B. B. Oakley, N.
510 Narang, P. Fratamico and W. C. J. R. Cray, *J. Food Prot.*, 2012, 75, 1548-1554.
- 511 12. Y. Arakawa, T. Sawada, K. Takatori, K.-I. Lee and Y. Hara-Kudo, *Biocontrol Sci.*, 2011, 16,
512 159-164.
- 513 13. A. Gill, A. Martinez-Perez, S. McIlwham and B. Blais, *J. Food Prot.*, 2012, 75, 827-837.
- 514 14. J. Bergan, A. B. Dyve Lingelem, R. Simm, T. Skotland and K. Sandvig, *Toxicon*, 2012, 60,
515 1085-1107.
- 516 15. U. Reischl, M. T. Youssef, J. Kilwinski, N. Lehn, W. L. Zhang, H. Karch and N. A.
517 Strockbine, *J. Clin. Microbiol.*, 2002, 40, 2555-2565.
- 518 16. O. Lazcka, F. J. D. Campo and F. X. Muñoz, *Biosensors Bioelectron.*, 2007, 22, 1205-1217.
- 519 17. V. Velusamy, K. Arshak, O. Korostynska, K. Oliwa and C. Adley, *Biotechnol. Adv.*, 2010,
520 28, 232-254.

- 521 18. J. Du, B. Zhu, X. Peng and X. Chen, *Small*, 2014.
- 522 19. S. M. Shawky, D. Bald and H. M. E. Azzazy, *Clin. Biochem.*, 2010, 43, 1163-1168.
- 523 20. D. Aili, P. Gryko, B. Sepulveda, J. A. G. Dick, N. Kirby, R. Heenan, L. Baltzer, B.
524 Liedberg, M. P. Ryan and M. M. Stevens, *Nano Lett.*, 2011, 11, 5564-5573.
- 525 21. K. Saha, S. S. Agasti, C. Kim, X. Li and V. M. Rotello, *Chem. Rev.*, 2012, 112, 2739-2779.
- 526 22. W. Zhao, W. Chiuman, M. A. Brook and Y. Li, *ChemBioChem*, 2007, 8, 727-731.
- 527 23. L. Yang and Y. Li, *Analyst*, 2006, 131, 394-401.
- 528 24. S.-H. Chen, K.-I. Lin, C.-Y. Tang, S.-L. Peng, Y.-C. Chuang, Y.-R. Lin, J.-P. Wang and C.-
529 S. Lin, *IEEE Trans. NanoBiosci.*, 2009, 8, 120-131.
- 530 25. V. Chegel, O. Rachkov, A. Lopatynskiy, S. Ishihara, I. Yanchuk, Y. Nemoto, J. P. Hill and
531 K. Ariga, *J. Phys. Chem. C*, 2011, 116, 2683-2690.
- 532 26. W. Zhao, M. A. Brook and Y. Li, *ChemBioChem*, 2008, 9, 2363-2371.
- 533 27. R. Jin, G. Wu, Z. Li, C. A. Mirkin and G. C. Schatz, *J. Am. Chem. Soc.*, 2003, 125, 1643-
534 1654.
- 535 28. W. Zhao, W. Chiuman, J. C. Lam, S. A. McManus, W. Chen, Y. Cui, R. Pelton, M. A.
536 Brook and Y. Li, *J. Am. Chem. Soc.*, 2008, 130, 3610-3618.
- 537 29. D. J. Bolton, *Foodborne Pathog. Dis*, 2010, 8, 357-365.
- 538 30. S. Derzelle, A. Grine, J. Madic, C. P. de Garam, N. Vingadassalon, F. Dilasser, E. Jamet and
539 F. Auvray, *Int. J. Food Microbiol.*, 2011, 151, 44-51.
- 540 31. M. Lin, H. Pei, F. Yang, C. Fan and X. Zuo, *Advanced Materials*, 2013, 25, 3490-3496.
- 541 32. V. Jasson, L. Jacxsens, P. Luning, A. Rajkovic and M. Uyttendaele, *Food Microbiol.*, 2010,
542 27, 710-730.
543



30x22mm (300 x 300 DPI)

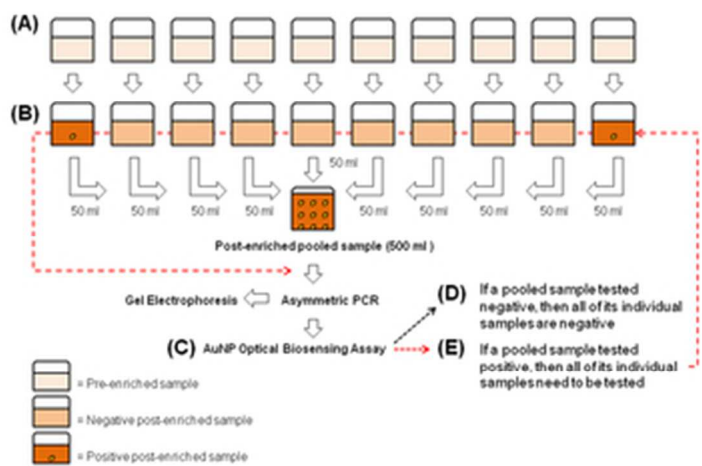


Figure 2

30x22mm (300 x 300 DPI)

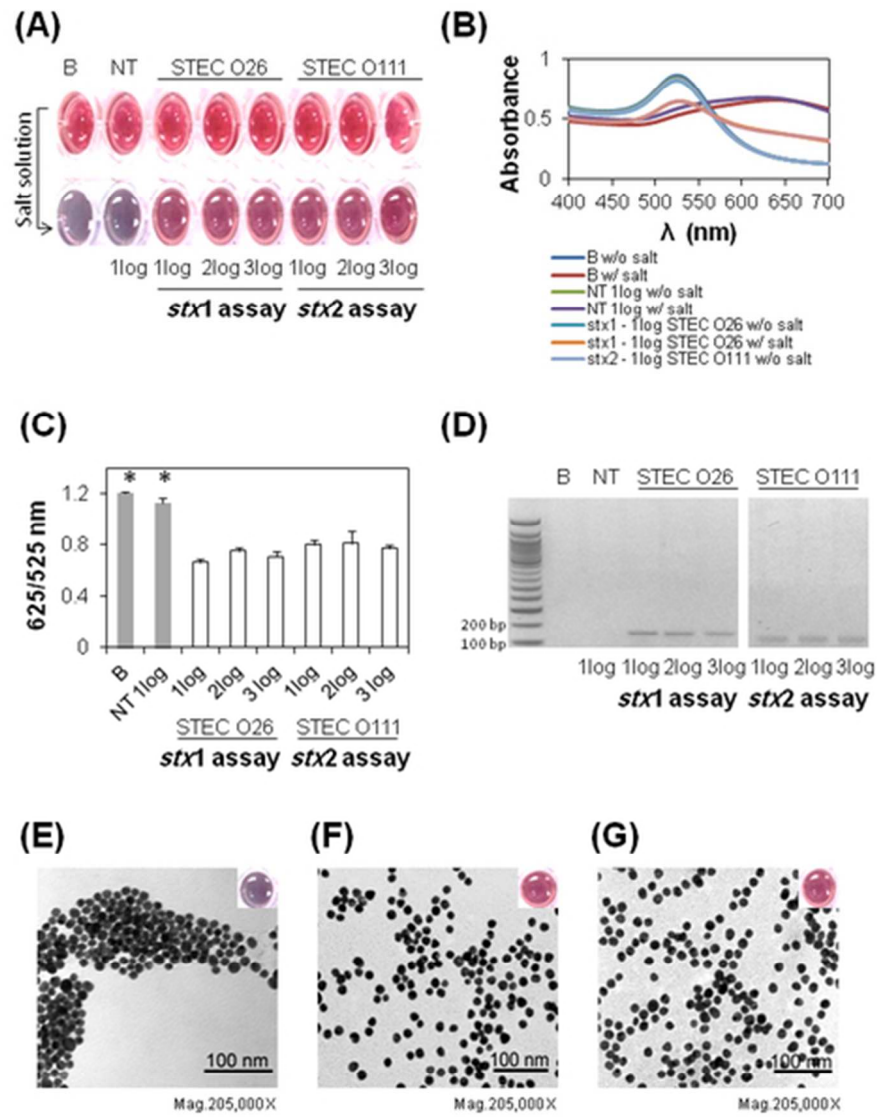


Figure 3

40x54mm (300 x 300 DPI)

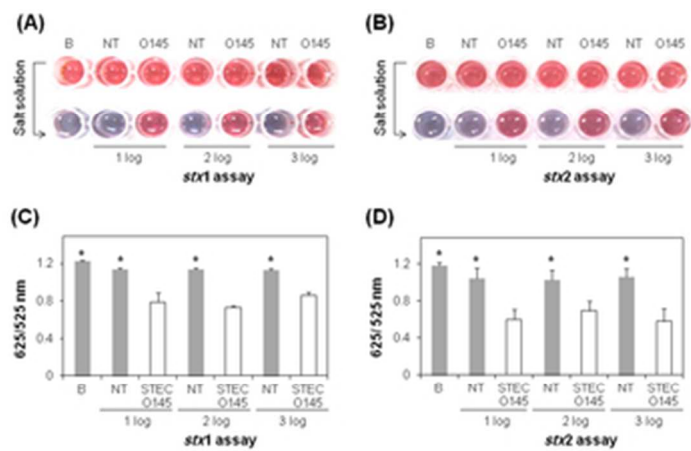


Figure 4

30x22mm (300 x 300 DPI)

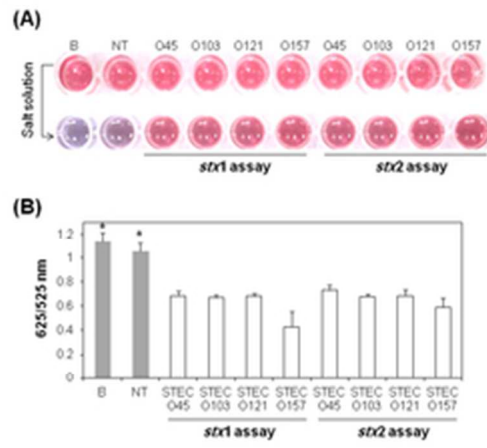


Figure 5

30x22mm (300 x 300 DPI)

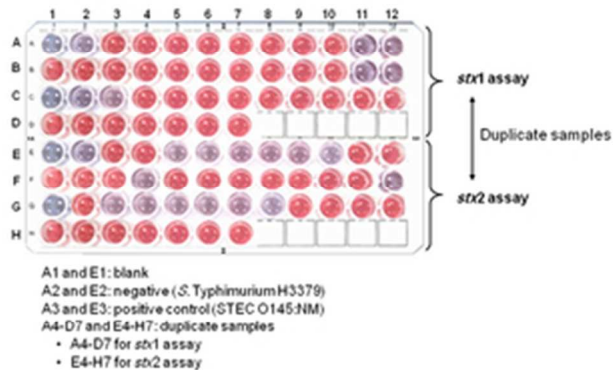


Figure 6

30x22mm (300 x 300 DPI)